

Measurement of the production cross-section of Z boson for the electron and muon decay channels with the ATLAS detector at $\sqrt{s} = 13$ TeV

10457059, Pau Petit Rosàs

Department of Physics and Astronomy, The University of Manchester

(Dated: April 24, 2024)

The cross-sections of the Z boson for the electron and muon decay channels are calculated using data from the ATLAS experiment. The proton-proton collision data was collected using an integrated luminosity of $10.06 fb^{-1}$ and $\sqrt{s} = 13$ TeV. Using Monte Carlo simulations of the $Z \rightarrow e^-e^+$ and $Z \rightarrow \mu^-\mu^+$ decays, sensible cuts were applied to the data to separate signal from background. The main source of uncertainty was identified to be the accuracy of these cuts, accounted in the systematic error. The cross-sections were measured to be $\sigma_{Z \rightarrow ee} = 1.974 \pm 0.001(stat.) \pm 0.016(syst.) \pm 0.034(lumi.)$ nb and $\sigma_{Z \rightarrow \mu\mu} = 1.955 \pm 0.001(stat.) \pm 0.021(syst.) \pm 0.033(lumi.)$ nb. These lie between 3 and 2 standard deviations from the Standard Model prediction respectively.

I. INTRODUCTION

According to the Standard Model, the Z boson is one of the three carriers of the electroweak force [1]. It has a range limit of around 10^{-18} m and a mass of 91 GeV [2]. The first observation of such bosons was made at CERN, using data from the Super Proton Synchrotron (SPS) accelerator, which then lead to the creation of the Large Electron-Positron collider to further study the properties of the weak interaction. This accelerator was then transformed to the current Large Hadron Collider (LHC). The Open Data from this collider consists of events from proton-proton collisions at center-of-mass energy $\sqrt{s} = 13$ TeV and integrated luminosity of $10.06 fb^{-1}$. This data was then used to calculate kinematic properties of the Z boson, such as the invariant mass or the production cross-section.

II. THEORY

A. Z boson decay channels and backgrounds

The Z boson interacts with leptons, quarks, and all the bosons except for gluons. Considering the lifetime stated above, it is not sufficient for it to be directly observed by the detector, which forces us to indirectly study it by observing the products of its decay. There are many decay channels for the Z boson, but only the electronic and muonic will be used, as the tau decay and others result in higher uncertainties due to their bigger masses. [3]. A Feynman diagram of the studied decays can be seen in Figure 1.

Furthermore, due to lepton universality, we expect the same production cross-section for both decays, as all leptons carry the same coupling strength and branching ratio to the weak force [4].

Many processes can be falsely identified as the result of the decay of the Z boson. Nevertheless, the background will be mainly dominated by the production

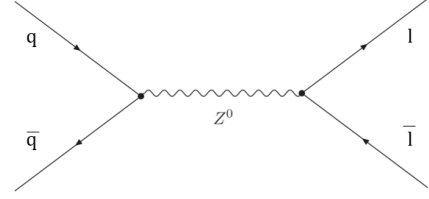


FIG. 1. Leading-order Feynman diagram for the process $q\bar{q} \rightarrow Z^0 \rightarrow l\bar{l}$ where $l\bar{l}$ can either be a e^-e^+ pair or a $\mu^-\mu^+$ pair.

of jets, a shower of partons, which are then misidentified as leptons in the detector, and the process of two W bosons decaying at the same time [5]. To take care of the first source, we will consider isolation variables, in particular, $ptcone30$ and $etcone20$, as high values of these variables are associated with jets [6]. To deal with the second contributor to the background we will take into account that the resulting leptons of the two W boson decays will have low momentum.

B. The ATLAS detector

The detector consists of different layers with an approximate circular symmetry, each layer designed to detect a particle. As electrons have less mass, they lose energy much faster due to Bremsstrahlung radiation, while muons are mainly defined by their tracks. The electrons are detected by the electromagnetic calorimeter and muons by the muon spectrometer [7].

In addition, the structure of ATLAS suggests using another coordinate system, the geometry of which can be seen in Figure 2. Instead of using the usual x, y, and z, we will be working with the transverse momentum p_t , the pseudorapidity η , and the azimuthal angle ϕ .

Finally, the structure of the detector itself defines the first cuts on the data. The electrons must be in the tracking region of the inner detector, $|\eta| < 2.47$, excluding the

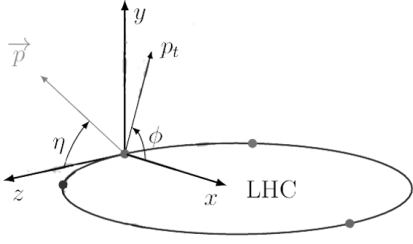


FIG. 2. LHC coordinate system

transition region between the barrel and the end-cap electromagnetic calorimeters, $-1.37 \leq |\eta| < 1.52$, and muons within $|\eta| < 2.4$ [5]. The cuts for electrons were found to be already implemented in the data sample, but not the one for muons. Consequently, the cuts for electrons were not implemented again.

C. Cross-section and Invariant mass

The invariant mass for a two-body system, m_{ll} can be rewritten in the new coordinate system as follows:

$$m_{ll}^2 = p_{T1}p_{T2}[\cosh(\eta_1 - \eta_2) - \cos(\phi_1 - \phi_2)] \quad (1)$$

where the subscripts 1, 2 denote the first and second lepton of the event, and the other symbols have the meanings defined in Section II.B. This kinematic variable will be used when considering the cuts to estimate our cross-sections.

Moreover, for each Z boson decay channel, we can find a cross-section using

$$\sigma_{Z \rightarrow ll} = \frac{N_{sel.} - N_{back.}}{\epsilon \int L dt} \quad (2)$$

where $N_{sel.}$ is the total number of events that pass our selection cuts, $N_{back.}$ is our estimate of the number of background events in the selected data sample and the integrated luminosity $\int L dt$ equals $10.06 fb^{-1}$. The efficiency ϵ is given by

$$\epsilon = \frac{N_{MC}}{N_{MCtotal}} \quad (3)$$

where N_{MC} is the total number of events from the Monte Carlo simulation that pass our cuts and $N_{MCtotal}$ is the total number of events of the simulation.

III. EVENT SELECTION

Using the properties of the products of the studied decays, the data was cut to separate signal from background. Apart from the cuts given by the structure

of the detector, the data was also cut to only consider events with two leptons from the same type -either electrons or muons- and opposite charges. Additionally, a total of four kinematic variables were considered to perform further cuts: the transverse momentum, the invariant mass (using Eq. 1), the $ptcone30$, and the $etcone20$. To decide where to place these cuts, both a stacked and a division plot of the simulated and real data were used. These plots were obtained using ROOT. An example can be seen in Figure 3. For the transverse momentum, particles with low momentum were cut, as they are highly unlikely to come from a Z decay. For the invariant mass, the studied range was between 60 and 120 GeV, as it is known that the invariant mass of the Z boson is around 90 GeV. For the isolation variables, high values of the $ptcone30$ and $etcone20$ were rejected, as they are most likely coming from jets. Furthermore, the plots of the transverse momentum and $ptcone30$ were split into the first and second lepton, to make more accurate cuts. The specific cuts can be found in Table I.

Selection Criteria		Z \rightarrow ee	Z \rightarrow $\mu\mu$
Identification Cuts	Lepton flavour	equal	
	Lepton charge	opposite	
	Lepton number	2	
	Pseudorapidity	—	< 2.4
Kinematic Cuts	p_{T1}	< 30 GeV	< 30 GeV
	p_{T2}	< 25 GeV	< 20 GeV
	Invariant mass	60 < m_{ll} < 120 GeV	
	$Ptcone30_1$	< 2.5 GeV	< 2 GeV
	$Ptcone30_2$	< 2 GeV	< 2 GeV
	Etcone20	< 5.5 GeV	< 4 GeV

TABLE I. Selection criteria applied to the electron and muon decay channel ATLAS data.

IV. UNCERTAINTIES

There are three main categories of error: statistical, systematic, and luminosity uncertainties. This last one is 1.7% and comes from the characteristics of the detector [8]. All three categories are stated separately in the final result. To estimate the systemic uncertainty, the one associated with particle and charge misidentification as well as the efficiency of our cuts, we vary them in a sensible range and calculate the new cross-sections. Using the upper-lower bounds method the error is then calculated. When varying the different kinematic variables cuts, we find that the cuts in $ptcone30$ are the ones that contribute the most to this uncertainty. Finally, as the histograms produced are Poisson distributions there is an associated statistical uncertainty to them. This can be found by propagating an error of \sqrt{N} , where N is the number of entries over bins.

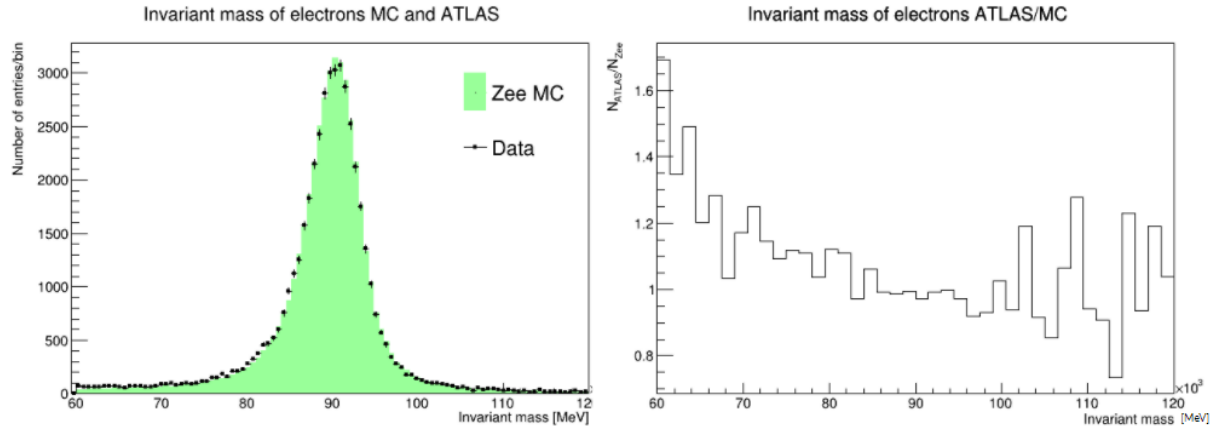


FIG. 3. Stacked plot (left) and division plot (right) of the invariant mass of electron decay channel from the Monte Carlo simulated data and ATLAS data.

V. RESULTS AND DISCUSSION

Putting everything together, Eq. 2 was used to calculate the production cross-section of the Z boson for the muon and electron decay channels. The variables in the equation were extracted from the histograms produced by ROOT, and the uncertainties were propagated as stated in the previous section. The results obtained are $\sigma_{Z \rightarrow ee} = 1.974 \pm 0.001(stat.) \pm 0.016(syst.) \pm 0.034(lumi.)$ nb and $\sigma_{Z \rightarrow \mu\mu} = 1.955 \pm 0.001(stat.) \pm 0.021(syst.) \pm 0.033(lumi.)$ nb. The first value lies between 3 standard deviations of the Standard Model prediction and 1 from the experimental literature value. The cross-section of the muon channel is consistent with the SM prediction by 2 standard deviations and by 1 standard deviation with the experimental literature value. The reference value is $\sigma_{Z \rightarrow ll} = 1.89 \pm 0.06$ [9].

As stated in Section II-A, the ratio, R , between the cross-section obtained using the electron and muon

channels is predicted to be 1 by the Standard Model. After sensibly propagating the uncertainties, we obtained a value of $R = 1.008 \pm 0.001(stat.) \pm 0.014(syst.)$, which agrees with the prediction within 1 standard deviation.

VI. CONCLUSIONS

Applying selection cuts to the ATLAS $\sqrt{s} = 13$ TeV data, the cross-section for the muon and electron decay channels for the Z boson were calculated and found to be $\sigma_{Z \rightarrow ee} = 1.974 \pm 0.001(stat.) \pm 0.016(syst.) \pm 0.034(lumi.)$ nb and $\sigma_{Z \rightarrow \mu\mu} = 1.955 \pm 0.001(stat.) \pm 0.021(syst.) \pm 0.033(lumi.)$ nb. The values agree within three and two standard deviations with the value of reference, predicted by the Standard Model. The values could be improved by using data-driven estimated background and making tighter cuts to the kinematic variables, more precisely exploring the pt_{cone30} . This would also reduce the systematic uncertainties of the obtained cross-sections.

-
- [1] S. Weinberg, A model for leptons, Physical Review Letters **19**, 1264 (1967).
 - [2] CERN, The z boson.
 - [3] Measurement of the tau lepton reconstruction and identification performance in the atlas experiment using pp collisions at $\sqrt{s} = 13$ tev, Tech. Rep. ATLAS-CONF-2017-029 (2017).
 - [4] M. Davier, Lepton universality, 25th SLAC Summer Institute on Particle Physics: Physics of leptons (1998).
 - [5] N. Zakharchuk, *Measurement of Z-boson production cross sections at $s = 13$ TeV and tt^- to Z-boson cross-section ratios with the ATLAS detector at the LHC*, Ph.D. thesis, University of Hamburg (2018).
 - [6] S. Moortgat, Lepton isolation using particle flow objects for the atlas detector, (2014).
 - [7] The atlas experiment at the cern large hadron collider, Journal of Instrumentation **3**.
 - [8] Luminosity determination in pp collisions at $\sqrt{s} = 13$ tev using the atlas detector at the lhc, ATLAS CONF Note (2019).
 - [9] Measurement of w^\pm and z-boson production cross sections in pp collisions at $\sqrt{s} = 13$ tev with the atlas detector, Physics Letters B **759**, 601 (2016).